A Model-Assisted Case Study Using Data from Open Guided Waves to Evaluate the Performance of Guided Wave-Based Structural Health Monitoring Systems

Kilian Tschöke[1](✉), Inka Mueller[2], Vittorio Memmolo[3], Ramanan Sridaran Venkat[4], Mikhail Golub[5], Artem Eremin[5], Maria Moix-Bonet[6], Kathrin Möllenhoff[7], Yevgeniya Lugovtsova[8], Jochen Moll[9], and Steffen Freitag[10]

[1] Fraunhofer Institute for Ceramic Technologies and Systems IKTS, Dresden, Germany
kilian.tschoeke@ikts.fraunhofer.de
[2] Bochum University of Applied Sciences, Bochum, Germany
[3] University of Naples "Federico II", Naples, Italy
[4] Saarland University, Saarbrücken, Germany
[5] Kuban State University, Krasnodar, Russia
[6] DLR Braunschweig, Braunschweig, Germany
[7] Heinrich Heine University Düsseldorf, Düsseldorf, Germany
[8] BAM, Berlin, Germany
[9] Goethe University Frankfurt, Frankfurt, Germany
[10] Karlsruhe Institute of Technology, Karlsruhe, Germany
https://www.ikts.fraunhofer.de/

Abstract. Reliability assessment of Structural Health Monitoring (SHM) systems poses new challenges pushing the research community to address many questions which are still open. For guided wave-based SHM it is not possible to evaluate the system performance without taking into account the target structure and applied system parameters. This range of variables would result in countless measurements. Factors like environmental conditions, structural dependencies and wave characteristics demand novel solutions for performance analysis of SHM systems compared to those relying on classical non-destructive evaluation. Such novel approaches typically require model-assisted investigations which may not only help to explain and understand performance assessment results but also enable complete studies without costly experiments. Within this contribution, a multi input multi output approach using a sparse transducer array permanently installed on a composite structure to excite and sense guided waves is considered. Firstly, the method and the analysis of path-based performance assessment are presented considering an open-access dataset from the Open Guided Wave platform. Then, a performance analysis of a guided wave-based SHM system using Probability of Detection is presented. To explain some unexpected results, the model-assisted investigations are used to understand the physical phenomena of wave propagation in the test specimen including the interaction with damage. Finally, issues and future steps in SHM systems' performance assessment and their development are discussed.

P. Rizzo and A. Milazzo (Eds.): EWSHM 2022, LNCE 254, pp. 937–944, 2023.
https://doi.org/10.1007/978-3-031-07258-1_94

1 Introduction

Structural Health Monitoring (SHM) is massively being investigated in many engineering fields in order to efficiently monitor critical structures, whose sudden and/or hidden failure gives rise to concern [1]. Among several techniques successfully implemented so far, those using ultrasonic guided waves (GWs) received much attention because they can propagate with relatively low attenuation over long distances and interact with a variety of defects emerging within a structure [2, 3]. Nonetheless, there is still a lack of industrial deployment of GW-based SHM systems and routine applications are far from being common. Among several factors preventing their massive implementation, a major concern comes from the lack of validation standards [4]. Despite the efforts of the SHM community [5], the performance assessment is still not trivial in the way to establish the reliability of an SHM system.

The standard procedures already established in the field of non-destructive testing, e.g. Probability of Detection (POD), cannot be fully transferred to the SHM systems due to many influencing parameters. In addition, testing the system reliability while including so many factors is time and cost consuming. That is where simulation comes into play, providing an useful tool to reduce or even replace measurements in order to look into system's performance [6]. However, despite recent breakthroughs achieved in this field, getting experimental results is still challenging when dealing with complex structures and needs further attention. In this context, the present paper shows different numerical techniques and model idealisation approaches in view of model-assisted performance assessment of GW-based SHM systems.

2 Path-Based Performance Assessment

A structure builds the basis for each SHM system. Even if two structures are made from the same material, the type of the structure will have a significant effect on the SHM system applied. Based on the structure, other defining factors are the requirements for the SHM system, like the type of damage under consideration, as well as environmental and operational conditions. The monitoring system itself is defined not only by the used type and amount of sensors building the measurement setup, but also and significantly by the data analytics, including method selection and possibilities of including training data. The aim of SHM is to monitor structural health using this defined system. For the applicability to industrial monitoring problems, it is necessary to take into account performance assessment. Therefore, the development of an SHM system must include performance assessment strategies like the Probability of Detection (POD). Evaluating the POD considers two parameters of the damage identification: the threshold for damage detection and the defect size. In a POD analysis the threshold value for damage detection is fixed, while several defect sizes are considered.

The POD is chosen in this work for performance assessment of SHM systems. The analysis requires two main inputs: the defect size a and the damage indicator $\hat{a}$ which is proportional/sensitive to the damage size. The damage indicator is obtained by comparing the signal response acquired in a damage-free and damaged state. In the scope of this work, the damage indicator *DI* for a specific actuator-sensor pair evaluates the energy difference between two structural states with:

$$DI = \sum_{k=1}^{k=N} (x_C(k) - x_B(k))^2 \quad (1)$$

where $x_B(k)$ represents the discrete signal response of the pristine state and $x_C(k)$ of the current state at time step k. N represents the maximum number of data points. A zero *DI* value indicates a healthy state, while increasing *DI* values correlate with growing defect sizes.

Moreover, no localization procedure is included, but the focus is on path-based POD analysis. The changing distance between damage and sensor network has a major influence during the damage identification process. Therefore, the effects of the damage-path on the POD are investigated in this work.

3 Theory of POD

Probability of Detection is one of the most suited approaches to assess the reliability of an SHM system, returning the minimum detectable size with a certain confidence level and an acceptable false call rate. It can be achieved with either hit/miss approach, where a binary decision is used to calculate the probability to detect a damage with a specific size, or $\hat{a}$ *vs.* a approach as used in classical NDT, where the relation between the signal response $\hat{a}$ and real damage size a is fitted to predict a regression curve, which is then used to derive the POD trend versus damage size. This latter technique is also well suited for *DI*-based SHM approaches, i.e. using *DI* instead of signal response to estimate the flaw size. Employing this approach, it is possible to estimate the signal response of an SHM system versus flaw dimension in a statistically meaningful way and, as such, the inherent POD as:

$$POD(a) = \int_{\hat{a}_{dec}}^{\infty} f_{\hat{a}|a}(\hat{a})\, d\hat{a} \quad (2)$$

where $f(\hat{a})$ is the normal probability density function around the predicted response.

However, the definition of the POD is still aleatory in the way the signal response is predicted through the linear regression. Hence, statistical bounds are used to establish the *95%* lower confidence, which is associated to the POD_{95}, which returns *97.5%* probability in stating that the actual POD is greater than that value. Once the POD95 is established, the flaw dimension which returns *90%* probability of detection is the critical damage dimension $a_{90|95}$, which can be detected by the system in a statistically significant way. The $a_{90|95}$ value can be assumed as the target of the system, namely the minimum detectable size, and compared to AI based identification performance. It is worth noting that the decision value can be set according to specific probability of false alarm (generally *10%*). Then the resulting $a_{90|95}$ can be assumed as the system target achievable at the cost of that false call ratio.

Furthermore, as will be shown in the later application example of this paper, laboratory investigations can be supported by simulations. As in the present case, numerical investigations are even used to interpret and understand the POD results of real laboratory measurements. This approach is therefore called model-assisted performance assessment of SHM systems.

4 Numerical Modelling

The method and the model-assisted analysis of path-based performance assessment presented are based on an open-access dataset from the Open Guided Wave platform [7]. The test specimen is a carbon fiber composite plate with an additional omega stringer. The geometry of the test specimen was provided as a CAD data set and its dimensions and material parameters correspond to those of the plate described in [8]. Furthermore, the setup of the modelling corresponds to that of the experiments, which is also described in [8]. This refers to the positions of the piezoelectric transducers, the positions, sizes and orientations of the artificial damage, as well as to the signals and frequencies of the performed pitch-catch measurements on this plate.

To save computational time, it is possible to chose a homogenized material model. Thus, a very fine meshing in the thickness direction of the plate can be avoided. From the stiffness matrix C_{ij} of a single ply, the lay-up of [45; 0; –45; 90; –45; 0; 45; 90] $_S$ and using the rotation over the z-axis for the angle θ, the stiffness matrices C_k' of the rotated plies k = 1; …; 16 could be determined by

$$C_{avg} = \sum_{k=1}^{16} \frac{h_k}{H} C_k' \tag{3}$$

where, h_i is the ply thickness and H the total thickness. The resulting homogenized stiffness matrix of the plate is

$$C_{avg}^{plate} = \begin{pmatrix} 56.6 & 20.1 & 5.6 & 0 & 0 & 0 \\ 20.1 & 56.6 & 5.6 & 0 & 0 & 0 \\ 5.6 & 5.6 & 11.2 & 0 & 0 & 0 \\ 0 & 0 & 0 & 3.6 & 0 & 0 \\ 0 & 0 & 0 & 0 & 3.6 & 0 \\ 0 & 0 & 0 & 0 & 0 & 18.2 \end{pmatrix} GPa$$

as well as of the stringer

$$C_{avg}^{stringer} = \begin{pmatrix} 59.1 & 23.1 & 3.4 & 0 & 0 & 6.8 \\ 23.1 & 86.6 & 3.6 & 0 & 0 & 6.8 \\ 3.4 & 3.6 & 9.6 & 0 & 0 & 0.1 \\ 0 & 0 & 0 & 4.8 & 0.2 & 0 \\ 0 & 0 & 0 & 0.2 & 4.4 & 0 \\ 6.8 & 6.8 & 0.1 & 0 & 0 & 24.9 \end{pmatrix} GPa$$

Since the later signal evaluation is done for the excitation frequency of *40* kHz, the validity of the homogenized model is compared to the multi-layered model at first.

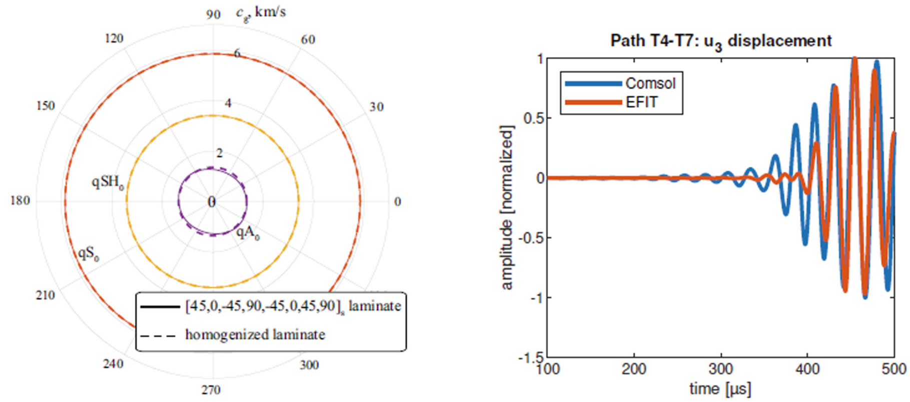

Fig. 1. Left: Comparison of homogenized and multi-layered models: group velocity angular dispersion curve for *40* kHz. Right: Exemplary comparison between COMSOL and EFIT: normalized out-of-plane displacement *u3* at the sensor position T7 with the excitation at T4.

Looking at the angular dispersion curve of the group velocity, one can see a high level of agreement between two models (Fig. 1, left), thus, allowing the use of the homogenized model for accurate numerical modelling.

The Elastodynamic Finite Integration Technique (EFIT) as well as the FEM software COMSOL are used for modelling the wave propagation. The EFIT method allows to model the complete wave field in heterogeneous, anisotropic materials and is based on staggered grids in space and time. Further details can be found in [9]. For the EFIT simulation a cartesian grid with a grid size of *1* mm was used for the whole specimen and the time step was *35.7* ns. The excitation was modelled as a force acting on the surface of the plate and the displacements were used as sensor signals. In COMSOL, the Solid Mechanics module was used to model the plate as well as the stringer, and the Electrostatics module was used to model the piezoelectric transducers. A free tetrahedral mesh was implemented using quadratic Serendipity elements for the Solid Module and quadratic elements for the Electrostatics module. The spatial step size was *3* mm and the time step size was *0.1* µs. A damage was modelled as an application of a metallic circular disc, as described in [8], where also the details on the experimental design and the positions of the damage can be found. For each pair of transducers mentioned, the damage-free condition was first simulated. Then the simulations were repeated with damage of different sizes. Differential signals were calculated from the signals received at the sensors and the damage indicators *DI* were calculated according to (1).

5 Results and Discussion

Again, it should be noted that the setup of the test specimen and the description of the experiments are given in [8]. Moreover, the simulation tools COMSOL and EFIT show a high level of agreement as can be seen in Fig. 1 (right) which shows the out-of-plane displacement at receiver location T7 after the *40* kHz burst excitation at position

T4. Both modelling environments reproduce the propagation speed of the guided wave modes very well.

In the next step, the calculation of the DIs according to [8] was also reproduced with the simulation data. Corresponding results are shown in Fig. 2 demonstrating a good agreement between the results of the experimental data and the simulation. It can be seen that the simulation data very accurately reproduce the behavior of the increasing *DI*s observed in the laboratory experiments for both selected actuator-sensor paths.

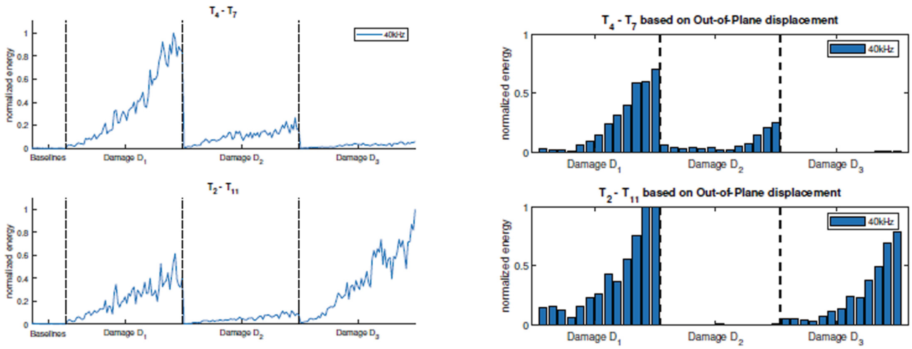

Fig. 2. Analysis of the normalized signal energy of the differential signal for two actuator-sensor paths as described in [8]. The horizontal axis is proportional to an increasing damage size for different damage locations (D_1, D_2, D_3). Left: Laboratory data based on the Open Guided Wave data set. Right: Data based on EFIT simulation. Both figures show the evaluation for DI_{Energy} and $f = 40$ kHz.

Based on the description in Section Theory of POD, the $a_{90|95}$ values were then calculated for each actuator-sensor path using the experimental data. A representation of the results for all 3 damage positions D_1, D_2 and D_3 is shown in Fig. 3, where $a_{90|95}$ is color-coded along different paths. The color scale ranges from red (small $a_{90|95}$ values) to blue (large $a_{90|95}$ values) where blue is for non-sensitive paths. Furthermore, we refer to [4], where an alternative possibility is described in detail to graphically represent the POD of a SHM network.

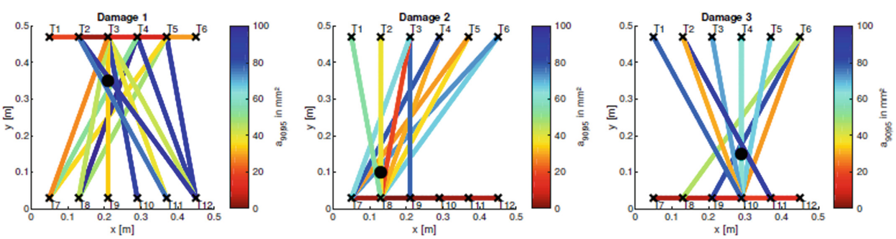

Fig. 3. Graphical representation of the $a_{90|95}$ values along different paths. The damage position is marked with a circle o, the transducers with crosses x. The figure shows the evaluation for DI_{Energy}, $f = 40$ kHz and $a_{dec} = 0.01$.

It can be seen for all 3 damage positions that the respective damage can be sensitively detected by transmission measurements. Interestingly, this plot also shows that there are both sensitive and non-sensitive paths in transmission measurements that cross the respective damage directly. Examples of such sensitive and non-sensitive paths are T4-T7 as well as T2-T11 for damage D1. Therefore, further COMSOL modelling was done to understand the behavior of the sensitive and non-sensitive paths more deeply.

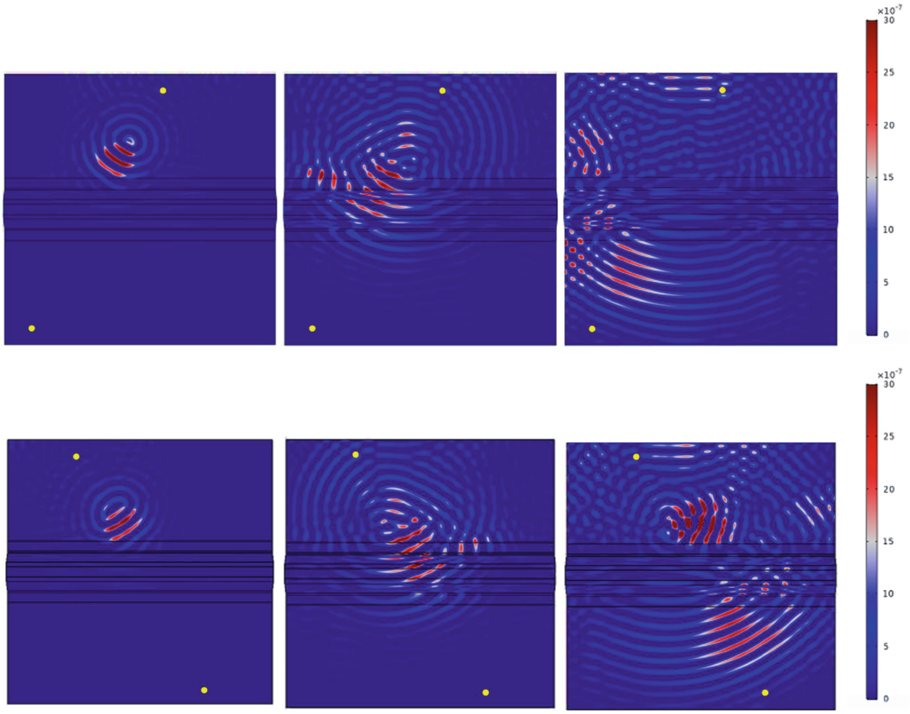

Fig. 4. The wave field of the differential signal (undamaged - damaged) for a damage of size *671* mm^2 at position D1. The time steps *150* µs*, 250* µs and *350* µs are shown from left to right, respectively. Top: Actuator-sensor path T4-T7. Bottom: Actuator-sensor path T2-T11.

Figure 4 shows the wave fields of the differential signals for the transducer paths T4-T7 and T2-T11. In both cases it can be seen that the propagation of the differential signal is directional along the respective path. It can also be seen for the time step of *350* µs that the differential signal is reflected at the left edge of the plate and this reflected part is received by the transducer T7 and thus the path T4-T7 is more sensitive to D1. In turn, such reflection is not visible at the right edge of the test specimen making the path T2-T11 less sensitive to D1.

6 Concluding Remarks

The presented modelling results show very clearly how simulations can support the understanding of experimental data and results of POD investigations. Moreover, POD is one potential solution for performance assessment of SHM systems. POD can be a tool to assess and optimize the parameters for a certain damage identification algorithm.

Acknowledgement. The authors gratefully acknowledge Dr. Daniel Kanzler for his valuable advice. The collaboration of the authors was supported by the German Research Foundation (DFG) within the scientific network "Towards a holistic quality assessment for guided wave-based SHM" (project number 424954879).

References

1. Boller, C., Chang, F.-K., Fujino, Y. (eds.): Encyclopedia of Structural Health Monitoring. Wiley, Hoboken (2009)
2. Mitra, M., Gopalakrishnan, S.: Guided wave based structural health monitoring: a review. Smart Mater. Struct. **25**(5), 053001 (2016)
3. Haynes, C., Todd, M.D., Flynn, E., Croxford, A.: Statistically-based damage detection in geometrically-complex structures using ultrasonic interrogation. Struct. Health Monit. **12**(2), 141–152 (2013). https://doi.org/10.1177/1475921712466756
4. Cawley, P.: Structural health monitoring: closing the gap between research and industrial deployment. Struct. Health Monit. **17**(5), 1225–1244 (2018)
5. Mueller, I., et al.: Performance assessment for active guided wave-based SHM systems - a case study using data from open guided waves. Struct. Health Monit. submitted - under review (2021)
6. Tschöke, K., et al.: Feasibility of model-assisted probability of detection principles or structural health monitoring systems based on guided waves for fibre-reinforced composites. IEEE Trans. Ultrason. Ferroelectr. Freq. Control **68**, 3156–3173(2021)
7. Moll, J., et al.: Open guided waves: online platform for ultrasonic guided wave measurements. Struct. Health Monit. **18**, 1903–1918 (2018)
8. Moll, J., et al.: Guided waves for damage detection in complex composite structures: the influence of omega stringer and different reference damage size. Appl. Sci. **10**, 1–21 (2020)
9. Tschöke, K., Gravenkamp, H.: On the numerical convergence and performance of different spatial discretization techniques for transient elastodynamic wave propagation problems. Wave Motion **82**, 62–85 (2018)